Proposal for Measuring the Parity Anomaly in a Topological Superconductor Ring

Chun-Xiao Liu, William S. Cole, and Jay D. Sau
Condensed Matter Theory Center and Joint Quantum Institute and Department of Physics, University of Maryland, College Park, Maryland 20742-4111, USA

(Received 18 April 2018; revised manuscript received 30 November 2018; published 22 March 2019)

A topological superconductor ring is uniquely characterized by a switch in the ground state fermion number parity upon insertion of one superconducting flux quantum—a direct consequence of the topological "parity anomaly." Despite the many other tantalizing signatures and applications of topological superconductors, this fundamental, defining property remains to be observed experimentally. Here we propose definitive detection of the fermion parity switch from the charging energy, temperature, and tunnel barrier dependence of the flux periodicity of two-terminal conductance of a floating superconductor ring. We extend the Ambegaokar-Eckern-Schön formalism for superconductors with a Coulomb charging energy to establish new explicit relationships between thermodynamic and transport properties of such a ring and the topological invariant of the superconductor. Crucially, we show that the topological contribution to the conductance oscillations can be isolated from Aharonov-Bohm oscillations of nontopological origin by their different dependence on the charging energy or barrier transparency.

DOI: 10.1103/PhysRevLett.122.117001

Topological superconductors (TSCs) are expected to support Majorana bound state excitations with non-Abelian statistics that might ultimately be harnessed for error-resistant quantum information processing [1–12]. Many simple, canonical examples of TSCs have been theoretically formulated in one- and two-dimensional time-reversal-breaking superconductors (i.e., in class D) [13–16], and several experiments now strongly suggest these have been realized in proximitized semiconductor nanowires among other systems [17–28]. However, despite the exciting progress that has been made, the experimental characterization of candidate TSCs still admits some stubborn controversy. To date, most evidence comes from local probes, such as zero-bias anomalies in transport or excess zero-energy density of states, which indicate the presence of bound states [17–28]. The origin of controversy, though, is that *any* bound state can always be decomposed, formally, into a pair of Majorana states so that even *prima facie* dramatic transport phenomena such as the recently observed quantized zero-bias peak or an anomalous temperature scaling of a peak over a large temperature range can arise from a plausible "quasi-Majorana" situation where the probe predominantly couples to just one Majorana component of a bound state that, nevertheless, is not of topological origin, and does not have exponential-in-length insensitivity to local perturbations [29–35].

Alternative methods to certify the existence of TSCs are therefore desirable. The fractional Josephson effect (where the current-flux relationship has a $2\Phi_0$ periodicity, with $\Phi_0 = h/2e$ being the SC flux quantum) at a junction between topological superconductors has a particular appeal [36,37]. But in practice measuring this effect requires the junction to remain in a fixed fermion parity state and therefore must be observed at frequencies higher than the inverse parity lifetime [14,15,36–39]. In turn, ac measurement leads to complications such as Landau-Zener transitions [40], which can yield a false positive in a topologically trivial state. The fractional Josephson effect, however, is merely an avatar of a more fundamental equilibrium topological property: the Z_2 ground state fermion parity of a TSC ring switches under the insertion of each SC flux quantum [36,41–46].

In this Letter we describe a definitive transport measurement of this fermion parity switch. The essential principle is that a Coulomb charging energy E_C promotes the parity anomaly into a genuine $2\Phi_0$ spectral periodicity [44] (this is also related to its role in "Majorana teleportation" [47]), and this can be distinguished from conventional Aharonov-Bohm (AB) oscillations (which share the same periodicity) since the latter have no such dependence on E_C. To investigate this situation quantitatively, we have generalized the Ambegaokar-Eckern-Schön (AES) model to the case of a topological superconductor ring tunnel coupling to external metallic leads. In this formalism we find that we can explicitly relate thermodynamic properties of the ring to the topological invariant, i.e., the ground state fermion parity.

The full Hamiltonian for the Coulomb blockaded normal-superconductor-normal (NSN) junction illustrated in Fig. 1 is

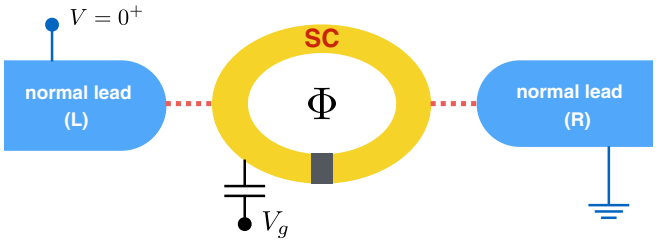

FIG. 1. Schematic of a proposed two-terminal transport experiment: a floating superconductor ring (yellow) is coupled to two normal metallic leads (blue). An infinitesimal bias voltage $V = 0^+$ is applied across the leads. An insulating junction (gray) is present in the middle of the ring, and the enclosed magnetic flux Φ varies continuously along with the energy $\delta(\Phi)$ of an Andreev bound state at the junction.

$$
\begin{aligned}
H &= H_{\mathrm{nw}} + H_g + H_C + H_{\mathrm{leads}} + H_T, \\
H_{\mathrm{nw}} &= \int \psi^\dagger \left(-\frac{\partial_x^2}{2m^*} - i\alpha\sigma_y\partial_x - \mu + V\sigma_z \right)\psi, \\
H_g &= -g \int \psi_\uparrow^\dagger \psi_\downarrow^\dagger \psi_\downarrow \psi_\uparrow, \\
H_C &= E_C \left(\int \psi^\dagger\psi - N_g \right)^2, \\
H_{\mathrm{leads}} &= \sum_{L,R} \int \psi_\alpha^\dagger \left(-\frac{\partial_x^2}{2m^*} - \mu_\alpha \right)\psi_\alpha, \\
H_T &= -t\psi_L^\dagger(L)\psi(r_L) - t\psi_R^\dagger(R)\psi(r_R) + \mathrm{H.c.}
\end{aligned}
\tag{1}
$$

H_{nw} is the semirealistic Majorana nanowire model [14,15] placed on a ring geometry, although we emphasize that the microscopic Hamiltonian for the SC ring will not be so essential in what follows. H_g describes an attractive, local pairing interaction, and H_C is the global charging energy relative to an induced charge N_g. The Coulomb blockaded SC ring is weakly coupled to external leads on the left (L) and right (R) side, with typical lead (H_{leads}) and coupling (H_T) Hamiltonians.

Large E_C and $E_C = 0$ limits.—The conductance in each of these cases can be understood qualitatively as shown in Fig. 2. We first consider large E_C [22,48] and an idealized low-energy limit (not essential for later) of the microscopic model: a single subgap state bound to the junction with energy $\delta(\Phi)$.The Bogoliubov–de Gennes (BdG) energy spectrum is Φ_0 periodic in both the topological and trivial cases, but the former has a parity switch and the latter does not [Figs. 2(a) and 2(b)]. In a conventional NSN Coulomb blockade, sharp zero-bias conductance peaks occur when the induced charge eN_g is tuned to degeneracy between charge states of the island separated by $2e$ and Andreev reflection (transferring a charge-$2e$ Cooper pair to the island) is enabled. If for any flux Φ the energy of the subgap state is *lower* than the charging energy of those two degenerate states [Figs. 2(c) and 2(d)], then Andreev

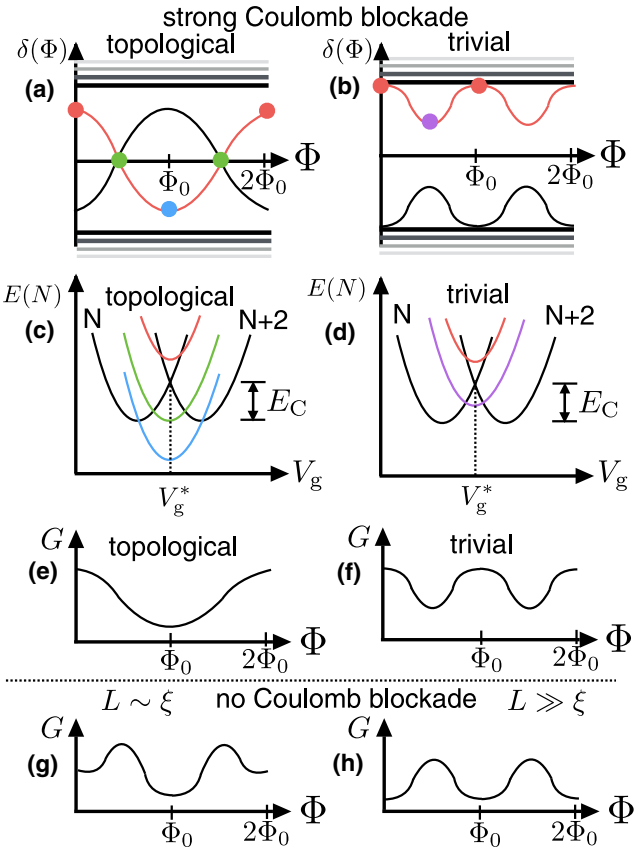

FIG. 2. Large and no charging energy limits. (a),(b) Energy spectra for the bound states at the junction of a topological or trivial SC ring. (c),(d) Evolution of the energy of the $N+1$ charge state as a function of the magnetic flux (Φ). Each color line corresponds to the color point in the spectra in (a) and (b), and V_g^* represents the resonance point at which the N and $N+2$ charge states are degenerate. (e),(f) Conductance for the NSN junction with strong Coulomb blockade. Topological (trivial) SC shows $2\Phi_0$ (Φ_0) periodicity. (g),(h) Conductance for the NSN junction with no Coulomb blockade. Here, the short (long) SC ring shows $2\Phi_0$ (Φ_0) periodicity in conductance, regardless of SC being topological or trivial.

conductance is suppressed as the island relaxes to the new nondegenerate ground state at this formerly resonant value of induced charge ($V_g = V_g^*$). Figures 2(e) and 2(f) show schematically that even though the BdG energy spectrum $\delta(\Phi)$ is Φ_0 periodic, the spectrum of H_C in the presence of this subgap state, and the corresponding conductance, need not be; in the topological case the conductance period is doubled.

By setting E_C to zero, on the other hand, there is no Coulomb blockade of Andreev processes. The conductance for the two-terminal junction with a floating superconductor is [49–51]

$$
G = \frac{e^2}{h} \frac{g_{LL}g_{RR} - g_{LR}g_{LR}}{g_{LL} + g_{RR} - g_{LR} - g_{LR}}. \tag{2}
$$

Here, g_{LL} (g_{RR}) is the dimensionless local conductance for the left (right) lead, while g_{LR} (g_{RL}) is the dimensionless conductance from the right (left) lead to the left (right) lead. In the short ring limit, the conductance for the NSN junction is always $2\Phi_0$ periodic, regardless of the SC ring being in the topological or trivial phase [Fig. 2(g)], as single-quasiparticle interference processes contribute to all $g_{\alpha\beta}$. In the long ring limit, single-quasiparticle interference is generally suppressed. As the transport coefficients are associated with the BdG energy spectrum only, which is Φ_0 periodic, conductance for a long SC ring is likewise Φ_0 periodic [Fig. 2(h)]. Thus, the conductance of the NSN junction absent from charging energy cannot distinguish between a topological or a trivial origin (i.e., arising from a short ring, or low-energy states due to disorder or order parameter fluctuations) of the doubled periodicity.

Generalized AES model.—To study the properties of the superconductor ring of Fig. 1 beyond the qualitative limits of the previous section, we analyze Eq. (1) in an imaginary-time path integral formulation in the form of AES [52]. Details are in Ref. [53], and we outline the procedure here. The partition function of the system can be written as $Z = \mathrm{Tr} e^{-\beta H} \equiv \int \mathcal{D}\bar{\psi}\mathcal{D}\psi e^{-S[\bar{\psi},\psi]}$. The infinite leads are replaced by self-energies $\Sigma_\alpha(\tau) = [-\Gamma_\alpha/\beta]/[\sin(\pi\tau/\beta)]$. For the quartic terms H_g and H_C, we perform the standard Hubbard-Stratonovich transformations to replace them with an imaginary-time-varying SC pairing potential $\Delta(x,\tau)e^{i\phi(x,\tau)}$ and an electrostatic potential $V(\tau)$ tracking total charge fluctuations, and to make the problem tractable, we focus on fluctuations around the saddle point with constant $\Delta(x,\tau) = \Delta_0$, valid for $T \ll \Delta_0$, and $\phi(x,\tau) = \phi(\tau)$. Note that the effect of the magnetic flux threading through the ring is now absorbed in H_{nw}.

To eliminate the ϕ dependence from the effective fermion Hamiltonian, we make a gauge transformation to the fermion fields $\psi(x,\tau) \to \psi' = \exp(i\phi/2)\psi$. However, we observe that this results in an atypical boundary condition for fermions: $\psi'(\beta) = -\exp(i\pi W)\psi'(0)$, where $W = \int_0^\beta d\tau(\partial_\tau\phi)/2\pi = [\phi(\beta) - \phi(0)]/2\pi$ is the integer winding number of the phase field. In other words, ψ' is antiperiodic or periodic in β depending on whether the winding number W is even or odd. This gauge transformation further results in an effective chemical potential variation $\delta\mu = i(\partial_\tau\phi/2 + V)$. Fixing $\delta\mu = 0$, in the same saddle point approximation, results in the Josephson relation $V(\tau) = -\partial_\tau\phi/2$ locking charge and phase fluctuations, after which we can finally integrate out the quadratic fermion fields.

Following these mostly standard manipulations, we begin to approach one of our central results: the only remaining degree of freedom in the effective action is the phase variable, and the partition function can be decomposed into discrete topological sectors indexed by W. Formally, then, the partition function is written as

$$Z = \sum_W Z_W = \sum_W Z_W^{\mathrm{BdG}} \int_W \mathcal{D}\phi e^{-S_W[\phi]}, \tag{3}$$

where, first, Z_W^{BdG} results from integrating out the ψ fields subject to the boundary condition stated above. Originating from the correspondence between boundary condition (and thus Fourier expansion in boson or fermion Matsubara frequencies) and winding number, we obtain that the topological invariant enters the partition function explicitly, depending on the parity of W,

$$Z_{\mathrm{even}W}^{\mathrm{BdG}} = \prod_{\varepsilon>0} 2\cosh\left(\frac{\beta\varepsilon}{2}\right), \tag{4}$$

$$Z_{\mathrm{odd}W}^{\mathrm{BdG}} = (\mathrm{sgnPf} H_{\mathrm{BdG}}) \prod_{\varepsilon>0} 2\sinh\left(\frac{\beta\varepsilon}{2}\right), \tag{5}$$

where H_{BdG} is the mean-field quadratic Hamiltonian appearing in the action after the Hubbard-Stratonovich transformation, written in the Majorana basis, and ε are its positive eigenvalues. It is useful at this point to note that there is *no* direct correspondence between winding number and the parity of occupied quasiparticle states, so this decomposition is conceptually distinct from prior works where the partition function is written as a sum of odd and even quasiparticle occupation parity sectors. We do recover, however, an equivalent partition function (see, e.g., Ref. [54]) in the appropriate $E_C = 0$ limit.

Next, the remaining effective action for the phase, $S_W[\phi] = S_W^0[\phi] + S_W^{\mathrm{leads}}[\phi]$, consists of the familiar "particle on a ring" (N.B., in imaginary time, rather than real space) with a topological term proportional to the induced charge,

$$S_W^0[\phi] = \int d\tau \frac{(\partial_\tau\phi)^2}{4E_C} - i\pi N_g W, \tag{6}$$

and a dissipative contribution arising from the tunnel coupling to the external leads,

$$\begin{aligned} S_W^{\mathrm{leads}}[\phi] &= -\frac{1}{2}\mathrm{Tr}\log(1 - G_{\mathrm{SC}}\Sigma) \\ &\simeq g_0 \int \frac{d\tau_1 d\tau_2}{\beta^2} \frac{1 - \cos[\phi(\tau_1) - \phi(\tau_2)]}{\sin^2[\pi(\tau_1 - \tau_2)/\beta]}, \end{aligned} \tag{7}$$

where $g_0 = (g_{LL} + g_{RR})/2$ is the dimensionless local conductance averaged over left and right leads. We have assumed that the tunneling strength between the SC island and the leads Γ_α is weak, and that the Green's function of the SC island $G_{\mathrm{SC}}(x,\tau)$ is local in both space and time [53].

Summarizing so far, we have derived an effective action in the form of the AES model, and in doing so we made manifest the relationship between the imaginary-time winding number of the effective phase degree of freedom and the

ground state parity of the superconductor, expressed as Kitaev's topological invariant [36]. The charging energy controls the relative contribution of different winding number sectors to the full partition function. Therefore, flux period doubling arising from the topological parity switch has explicit Coulomb dependence, whereas any conventional Aharanov-Bohm periodicity appears already in Z_0 with no dependence at all on E_C. In other words, topological and nontopological period doubling can be disentangled even in a device where the latter is present.

Measurement.—Like the partition function itself, any equilibrium observable can be expanded in W sectors and evaluated independently in each. To facilitate this, for each W we can take $\phi(\tau) = 2\pi W\tau/\beta + \delta\phi(\tau)$, where $\delta\phi(0) = \delta\phi(\beta)$, so all the winding is contained in the first part. With this substitution,

$$S_W^0[\phi] = \frac{\pi^2 W^2}{\beta E_C} - i\pi N_g W + \int d\tau \frac{(\partial_\tau \delta\phi)^2}{4E_C}, \quad (8)$$

which heavily suppresses large winding number contributions for intermediate temperatures $E_C \lesssim T \ll \Delta_0$. Continuing in this regime, we also obtain to zeroth order in $\delta\phi$ that $S_W^{\text{leads}} = 2g_0|W|$, so that, approximately,

$$Z_{\pm 1}/Z_0 \approx (\text{sgnPf}H_{\text{BdG}}) \prod_{\varepsilon>0} 2\tanh\left(\frac{\beta\varepsilon}{2}\right) \times \exp(\pm i\pi N_g) \exp\left(-\frac{\pi^2}{\beta E_C} - 2g_0\right), \quad (9)$$

and so any ground state parity dependence can be equivalently eliminated by (i) lowering E_C, (ii) increasing temperature, or (iii) increasing the barrier transparency and therefore g_0, all of which tend to favor a pinned phase ϕ.

To quadratic order in $\delta\phi$ we next calculate the zero-bias conductance of the device in Fig. 1 as [53,55]

$$G \approx g_0 \langle e^{i\phi(\beta/2) - i\phi(0)} \rangle \approx G_0 + (G_1 - G_0)\frac{Z_1}{Z_0} + (G_{-1} - G_0)\frac{Z_{-1}}{Z_0}, \quad (10)$$

up to exponentially small corrections in g_0 and $(\beta E_C)^{-1}$. Equations (9) and (10) illuminate the behavior of the weakly Coulomb blockaded SC ring. As the ground state parity of the SC ring is now contained in the ratio $Z_{\pm 1}/Z_0$, when the charging energy E_C goes to zero, this ratio is exponentially suppressed. Correspondingly, the conductance without Coulomb blockade cannot give any information about the ground state parity of the SC ring. Instead, the conductance without Coulomb blockade is fixed by the BdG spectrum and quasiparticle wave functions of the isolated ring. G_0 in Eq. (10) will be Φ_0 ($2\Phi_0$) periodic, when the length of the ring is long (short) compared to the coherence length and the AB effect is suppressed (prominent). This asymptotic behavior based on our partition function calculation is consistent with the discussion following Eq. (2).

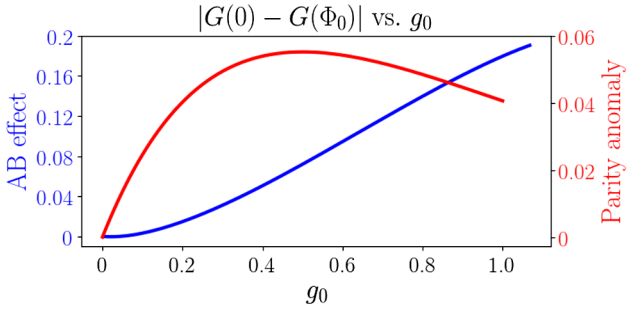

FIG. 3. Conductance difference $G(0) - G(\Phi_0)$ as a function of the barrier transparency characterized by g_0. For a short SC ring (no matter topologically trivial or nontrivial) with no charging energy, the conductance difference increases monotonically with barrier transparency (blue line). By contrast, for a TSC ring with charging energy, although increasing at low barrier transparency, the conductance difference will eventually decrease with barrier transparency when g_0 goes beyond some critical value ~0.5 (red line).

In Fig. 3, we plot the conductance difference after flux insertion, $G(0) - G(\Phi_0)$, as a function of the lead-SC interface conductance g_0 (since we are not in the strong Coulomb blockade limit, this is calculated at $N_g = 0$). A nonzero value of this conductance difference is a direct indication of $2\Phi_0$ periodicity, and g_0 is realistically tunable by a tunnel barrier. We consider first a short SC ring (it does not matter if the SC is topologically trivial or nontrivial) without Coulomb blockade and calculate the conductance using Eq. (2). The resulting conductance difference is shown by the blue line in Fig. 3. The signal of trivial AB-induced $2\Phi_0$ periodicity is monotonically increasing with the junction conductance g_0. For comparison, for the NSN junction with finite charging energy and topological SC ring, the conductance difference calculated by Eq. (10) is shown as the red line in Fig. 3. Note that although the conductance difference initially increases with small g_0, beyond some critical value $g_0 \simeq 0.5$, the signal of $2\Phi_0$ periodicity *decreases* with the conductance. This is because the large tunnel transparency effectively renormalizes the charging energy E_C to a smaller value and thus suppresses the parity anomaly-induced $2\Phi_0$ periodicity. Practically, if a decrease of $2\Phi_0$ periodicity with increasing tunnel conductance is observed experimentally, it would indicate a topologically nontrivial Coulomb blockaded superconductor. In reality, the signal may arise from both AB effect and parity anomaly, and the relative strength of the two is unknown *a priori*. We note, however, that the AB contribution can also be systematically suppressed by decreasing the junction transparency in the ring, and the parity anomaly contribution can be systematically increased by lowering the temperature.

Discussion.—Our proposal relates the two-terminal zero-bias conductance of the device in Fig. 1 to the fundamental equilibrium parity anomaly of the *bulk* topological superconductor, independent of the presence of Majorana modes or non-Abelian statistics. Accordingly, accidental, near-zero-energy ABS cannot alter this topological property of the ring to produce a false positive signature. In terms of feasibility, all the ingredients for this proposal are separately in place in previous experiments: (1) nanowire rings or "hashtags" demonstrating conventional Aharonov-Bohm oscilliations in the absence of superconductivity [56], (2) two-terminal proximity-SC islands, where Coulomb blockade can be tuned via the transparency of one of the barriers, and (3) robust Zeeman-tuned parity switches in Coulomb blockaded class D islands [57], indicating the absence of any substantial density of subgap states. It remains now to combine these ingredients. Although long parity lifetimes and protection from nonequilibrium quasiparticles will eventually be necessary for quantum information applications, they are not requirements for the definitive transport measurement of the parity anomaly we have discussed. Finally, from a theorist's perspective, we expect our generalization of the AES model, incorporating the mean-field topological invariant (sgn Pf H_{BdG}) and thereby exploring its beyond-mean-field consequences, could motivate related generalizations for floating topological superconductors and quantum dots in other symmetry classes.

We thank C.-K. Chiu for many helpful discussions. C.-X. L. was supported by Microsoft Station Q, and acknowledges the hospitality of the Kavli Institute of Theoretical Sciences at University of Chinese Academy of Sciences. W. S. C. was supported by LPS-MPO-CMTC. J. D. S. acknowledges support from the Alfred P. Sloan foundation and the National Science Foundation NSF DMR-1555135 (CAREER).

[1] C. Nayak, S. H. Simon, A. Stern, M. Freedman, and S. Das Sarma, Rev. Mod. Phys. **80**, 1083 (2008).
[2] J. Alicea, Rep. Prog. Phys. **75**, 076501 (2012).
[3] M. Leijnse and K. Flensberg, Semicond. Sci. Technol. **27**, 124003 (2012).
[4] C. Beenakker, Annu. Rev. Condens. Matter Phys. **4**, 113 (2013).
[5] T. D. Stanescu and S. Tewari, J. Phys. Condens. Matter **25**, 233201 (2013).
[6] J.-H. Jiang and S. Wu, J. Phys. Condens. Matter **25**, 055701 (2013).
[7] S. D. Sarma, M. Freedman, and C. Nayak, npj Quantum Inf. **1**, 15001 (2015).
[8] S. R. Elliott and M. Franz, Rev. Mod. Phys. **87**, 137 (2015).
[9] M. Sato and S. Fujimoto, J. Phys. Soc. Jpn. **85**, 072001 (2016).
[10] M. Sato and Y. Ando, Rep. Prog. Phys. **80**, 076501 (2017).
[11] R. Aguado, Riv. Nuovo Cimento **40**, 523 (2017).
[12] R. M. Lutchyn, E. P. A. M. Bakkers, L. P. Kouwenhoven, P. Krogstrup, C. M. Marcus, and Y. Oreg, Nat. Rev. Mater. **3**, 52 (2018).
[13] J. D. Sau, R. M. Lutchyn, S. Tewari, and S. Das Sarma, Phys. Rev. Lett. **104**, 040502 (2010).
[14] R. M. Lutchyn, J. D. Sau, and S. Das Sarma, Phys. Rev. Lett. **105**, 077001 (2010).
[15] Y. Oreg, G. Refael, and F. von Oppen, Phys. Rev. Lett. **105**, 177002 (2010).
[16] J. D. Sau, S. Tewari, R. M. Lutchyn, T. D. Stanescu, and S. Das Sarma, Phys. Rev. B **82**, 214509 (2010).
[17] V. Mourik, K. Zuo, S. M. Frolov, S. Plissard, E. P. A. M. Bakkers, and L. P. Kouwenhoven, Science **336**, 1003 (2012).
[18] A. Das, Y. Ronen, Y. Most, Y. Oreg, M. Heiblum, and H. Shtrikman, Nat. Phys. **8**, 887 (2012).
[19] M. T. Deng, C. L. Yu, G. Y. Huang, M. Larsson, P. Caroff, and H. Q. Xu, Nano Lett. **12**, 6414 (2012).
[20] H. O. H. Churchill, V. Fatemi, K. Grove-Rasmussen, M. T. Deng, P. Caroff, H. Q. Xu, and C. M. Marcus, Phys. Rev. B **87**, 241401 (2013).
[21] A. D. K. Finck, D. J. Van Harlingen, P. K. Mohseni, K. Jung, and X. Li, Phys. Rev. Lett. **110**, 126406 (2013).
[22] S. Albrecht, A. Higginbotham, M. Madsen, F. Kuemmeth, T. Jespersen, J. Nygård, P. Krogstrup, and C. Marcus, Nature (London) **531**, 206 (2016).
[23] J. Chen, P. Yu, J. Stenger, M. Hocevar, D. Car, S. R. Plissard, E. P. A. M. Bakkers, T. D. Stanescu, and S. M. Frolov, Sci. Adv. **3**, 9 (2017).
[24] M. T. Deng, S. Vaitiekenas, E. B. Hansen, J. Danon, M. Leijnse, K. Flensberg, J. Nygård, P. Krogstrup, and C. M. Marcus, Science **354**, 1557 (2016).
[25] H. Zhang *et al.*, Nat. Commun. **8**, 16025 (2017).
[26] Ö. Gül, H. Zhang, J. D. S. Bommer, M. W. A. de Moor, D. Car, S. R. Plissard, E. P. A. M. Bakkers, A. Geresdi, K. Watanabe, T. Taniguchi, and L. P. Kouwenhoven, Nat. Nanotechnol. **13**, 192 (2018).
[27] F. Nichele, A. C. C. Drachmann, A. M. Whiticar, E. C. T. O'Farrell, H. J. Suominen, A. Fornieri, T. Wang, G. C. Gardner, C. Thomas, A. T. Hatke, P. Krogstrup, M. J. Manfra, K. Flensberg, and C. M. Marcus, Phys. Rev. Lett. **119**, 136803 (2017).
[28] H. Zhang, C.-X. Liu, S. Gazibegovic, D. Xu, J. A. Logan, G. Wang, N. Van Loo, J. D. Bommer, M. W. De Moor, D. Car *et al.*, Nature (London) **556**, 74 (2018).
[29] G. Kells, D. Meidan, and P. W. Brouwer, Phys. Rev. B **86**, 100503 (2012).
[30] E. Prada, P. San-Jose, and R. Aguado, Phys. Rev. B **86**, 180503 (2012).
[31] C.-X. Liu, J. D. Sau, T. D. Stanescu, and S. Das Sarma, Phys. Rev. B **96**, 075161 (2017).
[32] C.-K. Chiu, J. D. Sau, and S. Das Sarma, Phys. Rev. B **96**, 054504 (2017).
[33] F. Setiawan, C.-X. Liu, J. D. Sau, and S. Das Sarma, Phys. Rev. B **96**, 184520 (2017).
[34] C.-X. Liu, J. D. Sau, and S. Das Sarma, Phys. Rev. B **97**, 214502 (2018).
[35] A. Vuik, B. Nijholt, A. Akhmerov, and M. Wimmer, arXiv:1806.02801.
[36] A. Y. Kitaev, Phys. Usp. **44**, 131 (2001).

[37] H.-J. Kwon, K. Sengupta, and V. M. Yakovenko, Eur. Phys. J. B **37**, 349 (2004).
[38] L. Fu and C. L. Kane, Phys. Rev. B **79**, 161408 (2009).
[39] B. Zocher, M. Horsdal, and B. Rosenow, Phys. Rev. Lett. **109**, 227001 (2012).
[40] J. D. Sau and F. Setiawan, Phys. Rev. B **95**, 060501 (2017).
[41] J. D. Sau, B. Swingle, and S. Tewari, Phys. Rev. B **92**, 020511 (2015).
[42] M. Cheng and R. Lutchyn, Phys. Rev. B **92**, 134516 (2015).
[43] M. Hell, K. Flensberg, and M. Leijnse, Phys. Rev. B **97**, 161401 (2018).
[44] S. Rubbert and A. R. Akhmerov, Phys. Rev. B **94**, 115430 (2016).
[45] K. M. Tripathi, S. Das, and S. Rao, Phys. Rev. Lett. **116**, 166401 (2016).
[46] C.-K. Chiu, J. D. Sau, and S. Das Sarma, Phys. Rev. B **97**, 035310 (2018).
[47] L. Fu, Phys. Rev. Lett. **104**, 056402 (2010).
[48] B. van Heck, R. M. Lutchyn, and L. I. Glazman, Phys. Rev. B **93**, 235431 (2016).
[49] Y. Takane and H. Ebisawa, J. Phys. Soc. Jpn. **61**, 1685 (1992).
[50] M. P. Anantram and S. Datta, Phys. Rev. B **53**, 16390 (1996).
[51] J. Ulrich and F. Hassler, Phys. Rev. B **92**, 075443 (2015).
[52] V. Ambegaokar, U. Eckern, and G. Schön, Phys. Rev. Lett. **48**, 1745 (1982).
[53] See Supplemental Material at http://link.aps.org/supplemental/10.1103/PhysRevLett.122.117001 for the complete derivation of the effective action of the NSN junction in the form of AES, and for the calculation of the corresponding conductance.
[54] C. W. J. Beenakker, D. I. Pikulin, T. Hyart, H. Schomerus, and J. P. Dahlhaus, Phys. Rev. Lett. **110**, 017003 (2013).
[55] E. Bascones, C. P. Herrero, F. Guinea, and G. Schön, Phys. Rev. B **61**, 16778 (2000).
[56] S. Gazibegovic *et al.*, Nature (London) **548**, 434 (2017).
[57] J. Shen, S. Heedt, F. Borsoi, B. van Heck, S. Gazibegovic, R. L. M. Op het Veld, D. Car, J. A. Logan, M. Pendharkar, S. J. J. Ramakers, G. Wang, D. Xu, D. Bouman, A. Geresdi, C. J. Palmstrøm, E. P. A. M. Bakkers, and L. P. Kouwenhoven, Nat. Commun. **9**, 4801 (2018).